

Research Article

Synthesis of Conductive PPy/SiO₂ Aerogels Nanocomposites by *In Situ* Polymerization of Pyrrole

Daliana Muller,¹ Geneviève K. Pinheiro,² Tatiana Bendo,¹ Alberto J. Gutiérrez Aguayo,² Guilherme M. O. Barra,¹ and Carlos R. Rambo²

¹Polymer and Composites Laboratory, Department of Mechanical Engineering, Federal University of Santa Catarina, 88040-900 Florianópolis, SC, Brazil

²Laboratory of Electrical Materials, Department of Electrical Engineering, Federal University of Santa Catarina, 88040-900 Florianópolis, SC, Brazil

Correspondence should be addressed to Carlos R. Rambo; carlos.rambo@ufsc.br

Received 11 January 2015; Revised 2 April 2015; Accepted 4 April 2015

Academic Editor: Ungyu Paik

Copyright © 2015 Daliana Muller et al. This is an open access article distributed under the Creative Commons Attribution License, which permits unrestricted use, distribution, and reproduction in any medium, provided the original work is properly cited.

Electrical conductive nanocomposite aerogels were synthesized through *in situ* oxidative polymerization of pyrrole (Py) using ammonium persulfate (APS) as an oxidizing agent in SiO₂ gels. The effect of Py concentration on the electrical conductivity and physical and morphological properties of aerogels SiO₂/PPy was evaluated. B.E.T. analysis indicated that the surface area of the composite SiO₂/PPy decreases with increasing concentration of Py. CHN analysis showed an increase in the amount of PPy, from 13 wt.% to 23 wt.%, with increasing concentration of pyrrole synthesis. FTIR-ATR analysis of the composites revealed bands in the region of 1500–1400 cm⁻¹, indicating the presence of the conductive polymer in the silica aerogel as well as the characteristic bands of Si-O-Si and Si-OH covalent bonds. TEM micrographs revealed the presence of particles of PPy with the increased size of the nanoparticles. The composites were successfully applied as passive components, in RC circuits, for low-pass frequency filters. The filters exhibited a cutoff frequency at approximately 435 Hz. The aerogels obtained in this work exhibited suitable electrical conductivity for use in various other applications in electronics.

1. Introduction

In recent years silica aerogels have been used as advanced material in various applications such as thermal insulation, electric batteries, nuclear waste storage, catalysis, acoustic insulation, and adsorbents [1]. These materials, which exhibit porosity between 95 and 99%, are comprised of a mesoporous nanostructure of interconnected particles having unique characteristics, such as high surface area, low density, and low thermal conductivity [1, 2]. Various strategies have been used to develop composites of silica aerogels with a variety of dispersed nanostructures, such as TiO₂, Pt, Au, RuO₂, SnO₂, and carbon nanotubes [3–5]. Therefore, it is possible to design new materials for a given application, combining the properties of silica aerogel with the desirable properties of the embedded material. Such class of composites is usually prepared through the dispersion of solid particles in a sol-

state SiO₂ matrix, before gelation, or through impregnation of suspensions into an already synthesized aerogel [1].

Recent works have reported interesting results concerning the incorporation of intrinsically conducting polymers (ICPs) into mesoporous silica (MCM-41) and SiO₂ aerogels [6–12]. Such class of nanocomposites exhibits a unique combination of chemical and physical properties, including a high specific surface area (SSA) and improved mechanical, thermal, and electrical properties, which make them suitable for a large variety of technological applications, such as sensors, photovoltaic devices, supercapacitors, catalysis, and electrorheological fluids [11–14]. Polymers such as polypyrrole (PPy), polyaniline (PAni), poly(3,4-ethylenedioxythiophene) (PEDOT), and polythiophene (PT) are studied most frequently, especially due to their stability at room temperature, high electrical conductivity, and ease of synthesis when compared to other ICPs [15, 16].

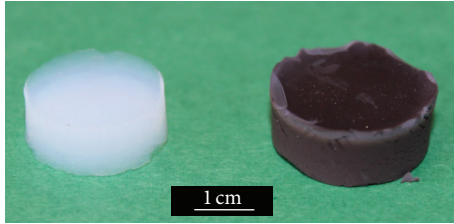


FIGURE 1: Photographs of SiO_2 (left) and SiO_2/PPy aerogels (right).

Several methods were developed to incorporate conductive polymers into aerogels, including dispersion of polyaniline nanofibers into silica sol prior to gelation [6], polymerization of aniline and chitosan in silica aerogels [7], and incorporation of polypyrrole into TiO_2 aerogels by sol-gel process [8]. Cheng et al. [10–12] produced mesoporous material with conducting polypyrrole confined in mesoporous silica through adsorption of pyrrole gas and subsequent oxidative polymerization. All *in situ* production methods showed to improve dispersion and uniformity of the dispersant in the aerogel matrix, resulting in homogenous and isotropic mesoporous nanocomposites.

In this work we report a one-step sol-gel process for the synthesis of nanocomposite SiO_2/PPy aerogels through *in situ* polymerization of different concentrations of pyrrole in silica gels. The nanostructure, composition, and electrical conductivity of the composites were also evaluated and the composites were applied as passive elements in low-pass frequency filters.

2. Experimental

Pyrrole monomer (Merk, analytic) was distilled under vacuum and stored at 8°C. Oxidizing agent ammonium persulfate (APS) (Vetec) was used as received. Polypyrrole was incorporated into SiO_2 aerogels through *in situ* polymerization of pyrrole as follows. The silica gels were prepared at room temperature using Py concentrations of 0.2–0.4 mol/L (0.23–0.46 g) in a solution (sol) containing 5.5 mL of ethanol and 2.5 mL of tetraethyl orthosilicate (TEOS) under stirring. A second solution was prepared containing 0.14 g of APS, 5.5 mL of ethanol, 3.5 mL of distilled water, and 0.2 mL of ammonium fluoride as catalyst. The two solutions were then mixed under stirring and placed into cylindrical PVC molds for gel formation.

After gelation, several solvent changes were performed to substitute ethanol by acetone in the alcogel. After solvent changes the gels were submitted to a drying/solvent extraction process under supercritical CO_2 (Supercritical System Quorum Technologies) at 80 bar, for four days. The formed SiO_2 aerogels are translucent white colored, as shown in Figure 1, left, while the SiO_2/PPy (prepared with 0.4 mol/L Py) aerogels exhibited a dark grey color (Figure 1, right) and were mechanically stable to handling.

Fourier transform infrared spectroscopy (FTIR) was performed with a Shimadzu, model IR PRESTIGE-2, instrument with an ATR (attenuated total reflectance) accessory, and

TABLE 1: Polypyrrole content and micropore volume of the SiO_2/PPy aerogels prepared with different initial pyrrole concentrations.

Composition	PPy-content (%)	Pore volume (cm^3/g)
SiO_2	0.0	2.0×10^{-1}
SiO_2/PPy [0.2]	13.1	1.0×10^{-1}
SiO_2/PPy [0.3]	17.5	8.9×10^{-2}
SiO_2/PPy [0.4]	23.4	7.8×10^{-2}

ZnSe crystal (ATR Smart Performance module). Spectra of pure silica aerogels, PPy, and nanocomposites were recorded in the range of 4000 to 600 cm^{-1} by accumulating 64 scans at a resolution of 4 cm^{-1} . Samples were previously powdered and analyzed in form of pellets. Specific surface area and total micropore volume were measured by B.E.T. method (Quantachrome Nova 1200E), using powdered samples. The amount of polypyrrole incorporated in the silica aerogels was determined by CHN analysis (PerkinElmer 2400 series III). X-ray diffraction (XRD) measurements were obtained at room temperature using a Philips diffractometer model X'Pert with $\text{CuK}\alpha$ radiation. Dried silica aerogels and SiO_2/PPy composites were placed on an aluminum plate and scanned over 2θ interval of 5° to 90° with steps of 1°/min. The nanomorphology of the aerogels was evaluated by transmission electron microscopy (TEM, JEOL-JEM 1011), operating at 100 kV. The samples for TEM analysis were prepared by dispersing powdered aerogels on carbon grids. The aerogels containing polypyrrole in three different concentrations were fragmented in smaller parts and placed between two flexible metal electrodes for electrical characterization and testing as low-pass filter components. The electrical conductivity of the SiO_2/PPy aerogels was measured using a high precision semiconductor analyzer (Agilent, B2912A). The aerogels were used as resistive elements (R) in RC circuit operating as frequency filters. The low-pass filters were tested by applying a sinusoidal wave form using a UniSource FG-8102 2 MHz Sweep Function Generator, and the results were registered using a Tektronix TDS2000C Digital Storage Oscilloscope. The stimulus for each filter was a sinusoidal signal with 2 V peak-to-peak and the time constant (τ , in seconds) was obtained using a ceramic capacitor ($C = 10 \text{ pF}$).

3. Results and Discussion

Table 1 shows the polypyrrole content determined by CHN and micropore volume obtained by B.E.T. of the SiO_2/PPy aerogels prepared with different initial pyrrole concentrations.

It is observed that, with increasing concentration of Py to be polymerized in the SiO_2 aerogel, the pore volume decreases by approximately an order of magnitude, which may be an indication that polymerization occurs between the pores of the aerogel. CHN analysis revealed, as expected, that the higher the concentration of pyrrole synthesis, the greater the conducting polymer amount in the silica aerogel.

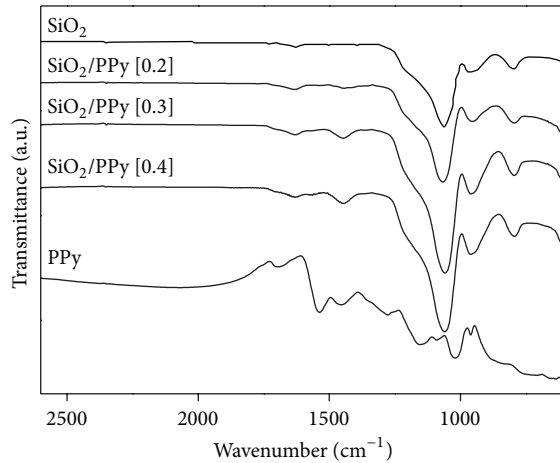


FIGURE 2: FTIR (ATR) spectra (transmittance) of SiO_2 and SiO_2/PPy nanocomposites prepared with different initial pyrrole concentrations.

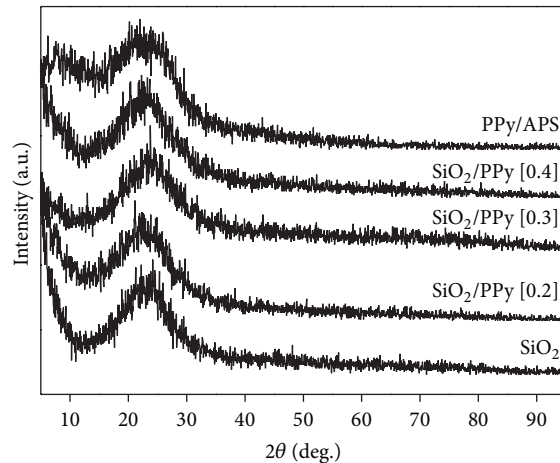


FIGURE 3: X-ray diffraction spectra of PPy, SiO_2 , and SiO_2/PPy aerogels prepared with different pyrrole concentrations.

Figure 2 shows FTIR spectra of silica aerogel and SiO_2/PPy nanocomposites produced with different concentrations of pyrrole. The spectrum of silica aerogel has three characteristic bands centered at 1060 , 960 , and 800 cm^{-1} . Intense vibrations of covalent Si-O bonds that appear mostly in the regions of 1000 - 1200 cm^{-1} can also be observed, indicating the existence of a dense chain of silica, in which the oxygen atoms play the role of bridging each of the two silicon sites. Another characteristic region appears around 795 cm^{-1} , which is related to the symmetric stretching of Si-O-Si bonds [17]. The vibrations of the Si-OH bond can be visualized in the region of 796 cm^{-1} .

After polymerization of pyrrole in the silica aerogels, the composites exhibit a band around 1460 cm^{-1} , related to the C-N bond of polypyrrole [18]. With enhancing of initial pyrrole concentration in the synthesis of the nanocomposites, the intensity of this band increased, indicating the increasing

content of polypyrrole in the aerogels, as previously observed in Table 1.

Figure 3 shows the X-ray diffractograms of SiO_2 and SiO_2/PPy aerogels produced with different initial Py concentrations.

The XRD spectrum of PPy exhibits no defined narrow diffraction peaks, but a broad halo at 2θ around 25° , characteristic of amorphous polypyrrole [19]. The broad peak centered between $2\theta = 20^\circ$ - 30° in the SiO_2 spectrum is characteristic of amorphous nano- SiO_2 [20]. The structure of silica matrix was not significantly modified; that is, no peak shift is observed, in the SiO_2/PPy composites, which also confirms the results obtained by FTIR.

Figure 4 shows TEM micrographs of SiO_2 aerogel and SiO_2/PPy nanocomposites prepared with different initial pyrrole concentrations.

It can be seen that the silica aerogel (Figures 4(a) and 4(b)) presents interconnected particles with diameters between 10 and 20 nm , typical of this class of material [21]. The amorphous structure of the SiO_2 particles is confirmed by the electron diffraction halo (insert in Figure 4(a)). As the concentration of pyrrole in a silica aerogel increases, there is an increase in particle size of the composites (Figures 4(c) to 4(e)). After *in situ* polymerization of pyrrole in the silica aerogel, clusters randomly distributed in the aerogel matrix were formed, not altering its nanostructure. Similar observations were reported by Harrel et al. [22].

Figure 5 shows the specific surface area and the electrical conductivity of the SiO_2 and SiO_2/PPy aerogels in function of initial pyrrole content.

The B.E.T. analysis revealed that the surface area of the composite SiO_2/PPy decreases with increasing concentration of Py. A significant reduction in the surface area of the composite between 48 and 65% , with the concentration of pyrrole during synthesis of aerogel, was observed. While SiO_2 aerogels exhibited SSA of $540\text{ m}^2/\text{g}$, the SiO_2/PPy aerogels exhibited surface areas in the range between 188 and $259\text{ m}^2/\text{g}$. This decrease was a result of the presence of agglomerated particles incorporated in the silica aerogel. Despite this decrease, the nanocomposites showed high surface area, at least the half, when compared to pure SiO_2 aerogel and to other SiO_2 -based aerogels [23]. The amount and dispersion of polypyrrole in the silica aerogel influenced the electrical conductivity of the nanocomposites. The higher the initial Py concentration in the gels was, and hence the polymer content after synthesis, the higher the electrical conductivity was achieved in the SiO_2/PPy aerogels. The aerogels exhibited values of conductivity close to a semiconductor material. Comparing SiO_2/PPy composites with the silica aerogel, there is an increase in conductivity of three orders of magnitude. This can be explained by the small amount of polymerized polypyrrole in the aerogel matrix, hindering the contact between particles of polypyrrole. As the Py concentration increases, more continuously conducting pathways are formed, leading to an increase in the conductivity.

Figure 6 shows the performance of the low-pass filters. The frequency range was limited for the signal generator resolution. All SiO_2/PPy composites exhibit cutoff frequencies

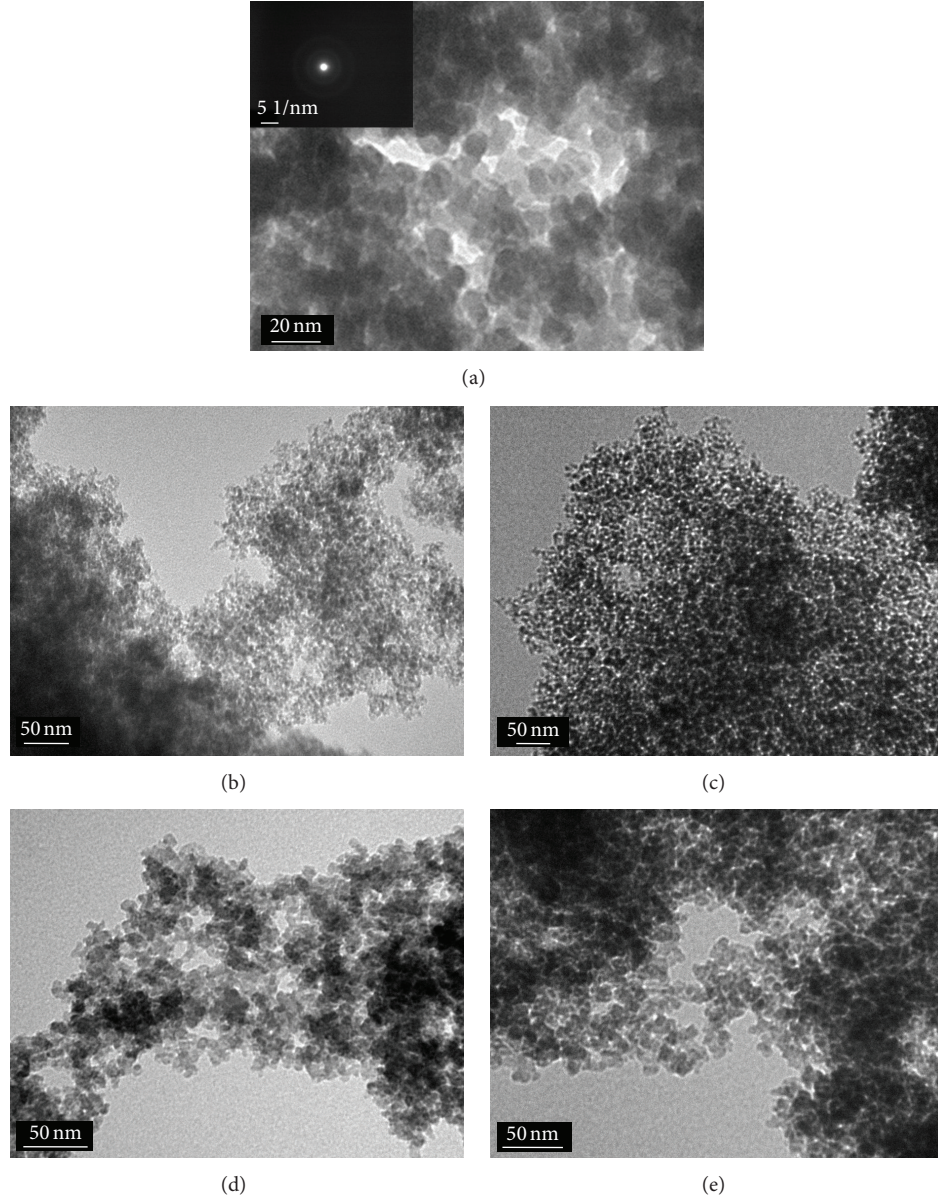


FIGURE 4: TEM micrographs of SiO_2 aerogel (a and b) and SiO_2/PPy nanocomposites prepared with different initial pyrrole concentrations: (c) 0.2 mol/L, (d) 0.3 mol/L, and (e) 0.4 mol/L. Insert in (a) is an electron diffraction pattern of a SiO_2 particle.

of around 435 Hz. Signal attenuation is also present for the composites, ranging from 30 to 50%, which indicates losses, probably due to the electrodes-sample contact resistance. The obtained time constants for the RC circuits were 6.8×10^{-4} , 2.3×10^{-4} , and 5.2×10^{-5} , for the composites prepared with Py concentrations of 0.2, 0.3, and 0.4 mol/L, respectively.

4. Conclusion

Electrical conductive SiO_2/PPy aerogels were prepared by *in situ* polymerization of pyrrole in SiO_2 aerogels. The SiO_2/PPy aerogels exhibit higher conductivity approximately three

orders of magnitude compared to pure silica aerogel. The polymerization of polypyrrole on silica aerogel resulted in aerogels with lower B.E.T. specific surface area and larger particle sizes, but no significant changes in the structure and typical morphology of the aerogels. The electrical conductivity of the mesoporous nanocomposites produced here was suitable for application as passive component in low-pass frequency filters.

Conflict of Interests

The authors declare that there is no conflict of interests regarding the publication of this paper.

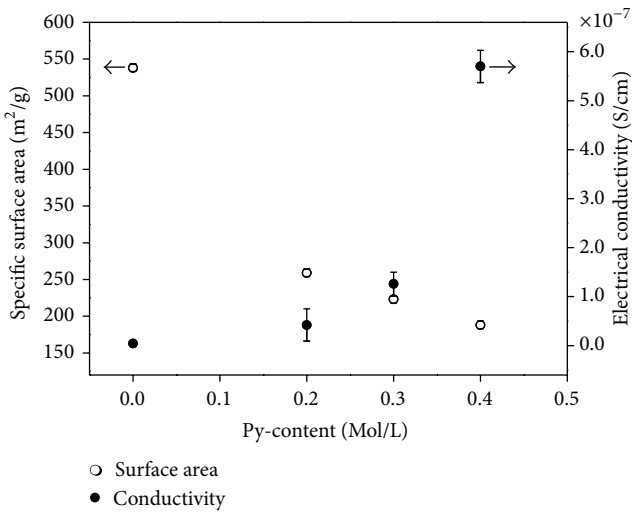


FIGURE 5: Specific surface area and the electrical conductivity of the SiO_2 and SiO_2/PPy aerogels in function of initial pyrrole content.

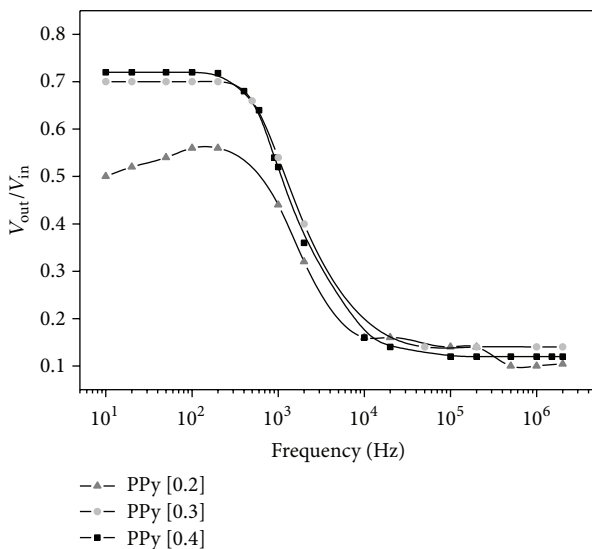


FIGURE 6: Performance curve ($V_{\text{out}}/V_{\text{in}}$ versus frequency) of low-pass frequency filters mounted with SiO_2/PPy composites with different initial pyrrole concentrations.

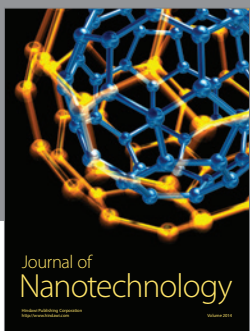
Acknowledgments

The authors thank the National Council for Scientific and Technological Development (CNPq, Brazil) and Coordination for the Improvement of Higher Level Personnel (CAPES, Brazil) for the financial support. Central Laboratory of Electronic Microscopy (LCME-UFSC) is also acknowledged.

References

- [1] J. L. Gurav, I.-K. Jung, H.-H. Park, E. S. Kang, and D. Y. Nadargi, "Silica aerogel: synthesis and applications," *Journal of Nanomaterials*, vol. 2010, Article ID 409310, 11 pages, 2010.
- [2] Z. Ulker, I. Erucar, S. Keskin, and C. Erkey, "Novel nanostructured composites of silica aerogels with a metal organic framework," *Microporous and Mesoporous Materials*, vol. 170, pp. 352–358, 2013.
- [3] M. N. P. Weerasinghe and K. J. Klabunde, "Chromium oxide loaded silica aerogels: novel visible light photocatalytic materials for environmental remediation," *Journal of Photochemistry and Photobiology A: Chemistry*, vol. 254, pp. 62–70, 2013.
- [4] H. Ren and L. Zhang, "In situ growth approach for preparation of Au nanoparticle-doped silica aerogel," *Colloids and Surfaces A*, vol. 372, no. 1-3, pp. 98–101, 2010.
- [5] S. V. Ingale, P. U. Sastry, P. B. Wagh et al., "Synthesis and micro structural investigations of titania-silica nano composite aerogels," *Materials Chemistry and Physics*, vol. 135, no. 2-3, pp. 497–502, 2012.
- [6] D. J. Boday, B. Muriithi, R. J. Stover, and D. A. Loy, "Polyaniline nanofiber-silica composite aerogels," *Journal of Non-Crystalline Solids*, vol. 358, no. 12-13, pp. 1575–1580, 2012.
- [7] S. Zhao, H. Xu, L. Wang, P. Zhu, W. M. Risen Jr., and J. William Suggs, "Synthesis of novel chitaline-silica aerogels with spontaneous Au and Ag nanoparticles formation in aerogels matrix," *Microporous and Mesoporous Materials*, vol. 171, pp. 147–155, 2013.
- [8] J.-D. Kwon, P.-H. Kim, J.-H. Keum, and J. S. Kim, "Polypyrrole/titania hybrids: synthetic variation and test for the photovoltaic materials," *Solar Energy Materials and Solar Cells*, vol. 83, no. 2-3, pp. 311–321, 2004.
- [9] Q. Cheng, V. Pavlinek, C. Li, A. Lengalova, Y. He, and P. Saha, "Synthesis and characterization of new mesoporous material with conducting polypyrrole confined in mesoporous silica," *Materials Chemistry and Physics*, vol. 98, no. 2-3, pp. 504–508, 2006.
- [10] L. Kavan, J. Rathouský, M. Grätzel, V. Shklover, and A. Zukal, "Mesoporous thin film TiO_2 electrodes," *Microporous and Mesoporous Materials*, vol. 44-45, pp. 653–659, 2001.
- [11] Q. Cheng, V. Pavlinek, A. Lengalova, C. Li, Y. He, and P. Saha, "Conducting polypyrrole confined in ordered mesoporous silica SBA-15 channels: preparation and its electrorheology," *Microporous and Mesoporous Materials*, vol. 93, no. 1-3, pp. 263–269, 2006.
- [12] Q. Cheng, V. Pavlinek, A. Lengalova, C. Li, T. Belza, and P. Saha, "Electrorheological properties of new mesoporous material with conducting polypyrrole in mesoporous silica," *Microporous and Mesoporous Materials*, vol. 94, no. 1-3, pp. 193–199, 2006.
- [13] T. Yamata, H.-S. Zhou, H. Uchida et al., "Surface photovoltage NO gas sensor with properties dependent on the structure of the self-ordered mesoporous silicate film," *Advanced Materials*, vol. 14, no. 11, pp. 812–815, 2002.
- [14] H. Kim and B. N. Popov, "Characterization of hydrous ruthe-nium oxide/carbon nanocomposite supercapacitors prepared by a colloidal method," *Journal of Power Sources*, vol. 104, no. 1, pp. 52–61, 2002.
- [15] Y. Lu, A. Pich, H.-J. P. Adler, G. Wang, D. Rais, and S. Nešpůrek, "Composite polypyrrole-containing particles and electrical properties of thin films prepared therefrom," *Polymer*, vol. 49, no. 23, pp. 5002–5012, 2008.
- [16] Y. Yang, Y. Chu, F. Yang, and Y. Zhang, "Uniform hollow conductive polymer microspheres synthesized with the sulfonated polystyrene template," *Materials Chemistry and Physics*, vol. 92, no. 1, pp. 164–171, 2005.

- [17] R. Al-Oweini and H. El-Rassy, "Synthesis and characterization by FTIR spectroscopy of silica aerogels prepared using several Si(OR)_4 and $\text{R}'\text{Si(OR')}_3$ precursors," *Journal of Molecular Structure*, vol. 919, no. 1–3, pp. 140–145, 2009.
- [18] M. Omastová, M. Trchová, J. Kovářová, and J. Stejskal, "Synthesis and structural study of polypyrroles prepared in the presence of surfactants," *Synthetic Metals*, vol. 138, no. 3, pp. 447–455, 2003.
- [19] R. E. Partch, S. G. Gangoli, E. Matijević, W. Cai, and S. Arajs, "Conducting polymer composites: I. Surface-induced polymerization of pyrrole on iron(III) and cerium(IV) oxide particles," *Journal of Colloid and Interface Science*, vol. 144, no. 1, pp. 27–35, 1991.
- [20] N. Thuadaij and A. Nuntiya, "Preparation of nanosilica powder from rice husk ash by precipitation method," *Chiang Mai Journal of Science*, vol. 35, no. 1, pp. 206–211, 2008.
- [21] C.-M. Wu, S.-Y. Lin, and H.-L. Chen, "Structure of a monolithic silica aerogel prepared from a short-chain ionic liquid," *Microporous and Mesoporous Materials*, vol. 156, pp. 189–195, 2012.
- [22] J. Harrelid, H. P. Wong, B. C. Dave, B. Dunn, and L. F. Nazar, "Synthesis and properties of polypyrrole-vanadium oxide hybrid aerogels," *Journal of Non-Crystalline Solids*, vol. 225, no. 1–3, pp. 319–324, 1998.
- [23] Q. Tang and T. Wang, "Preparation of silica aerogel from rice hull ash by supercritical carbon dioxide drying," *The Journal of Supercritical Fluids*, vol. 35, no. 1, pp. 91–94, 2005.



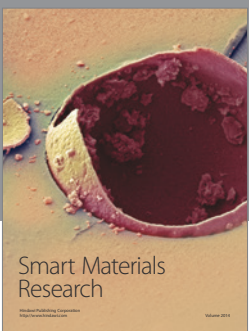
Journal of
Nanotechnology



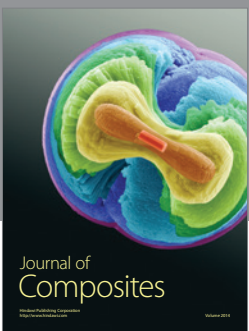
International Journal of
Corrosion



International Journal of
Polymer Science



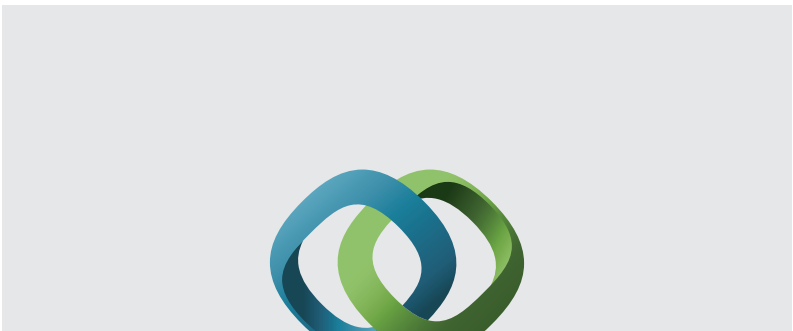
Smart Materials
Research



Journal of
Composites

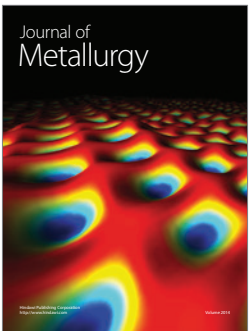


BioMed
Research International



Hindawi

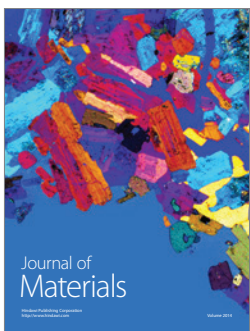
Submit your manuscripts at
<http://www.hindawi.com>



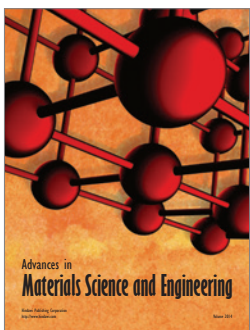
Journal of
Metallurgy



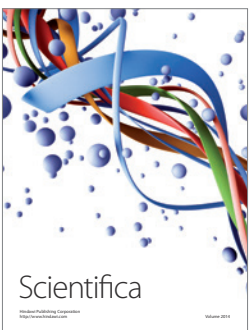
Journal of
Nanoparticles



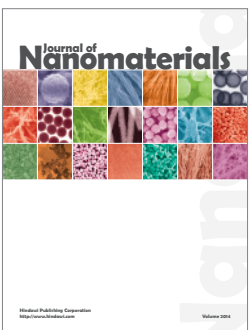
Journal of
Materials



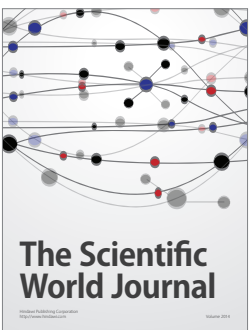
Advances in
Materials Science and Engineering



Scientifica



Journal of
Nanomaterials



The Scientific
World Journal



International Journal of
Biomaterials



Journal of
Nanoscience



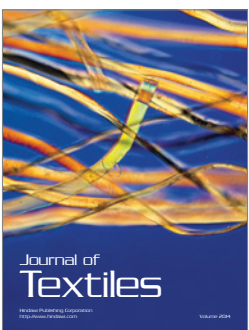
Journal of
Coatings



Journal of
Crystallography



Journal of
Ceramics



Journal of
Textiles